



Figures and figure supplements

Tumor suppression in basal keratinocytes via dual non-cell-autonomous functions of a Na,K-ATPase beta subunit

Julia Hatzold et al

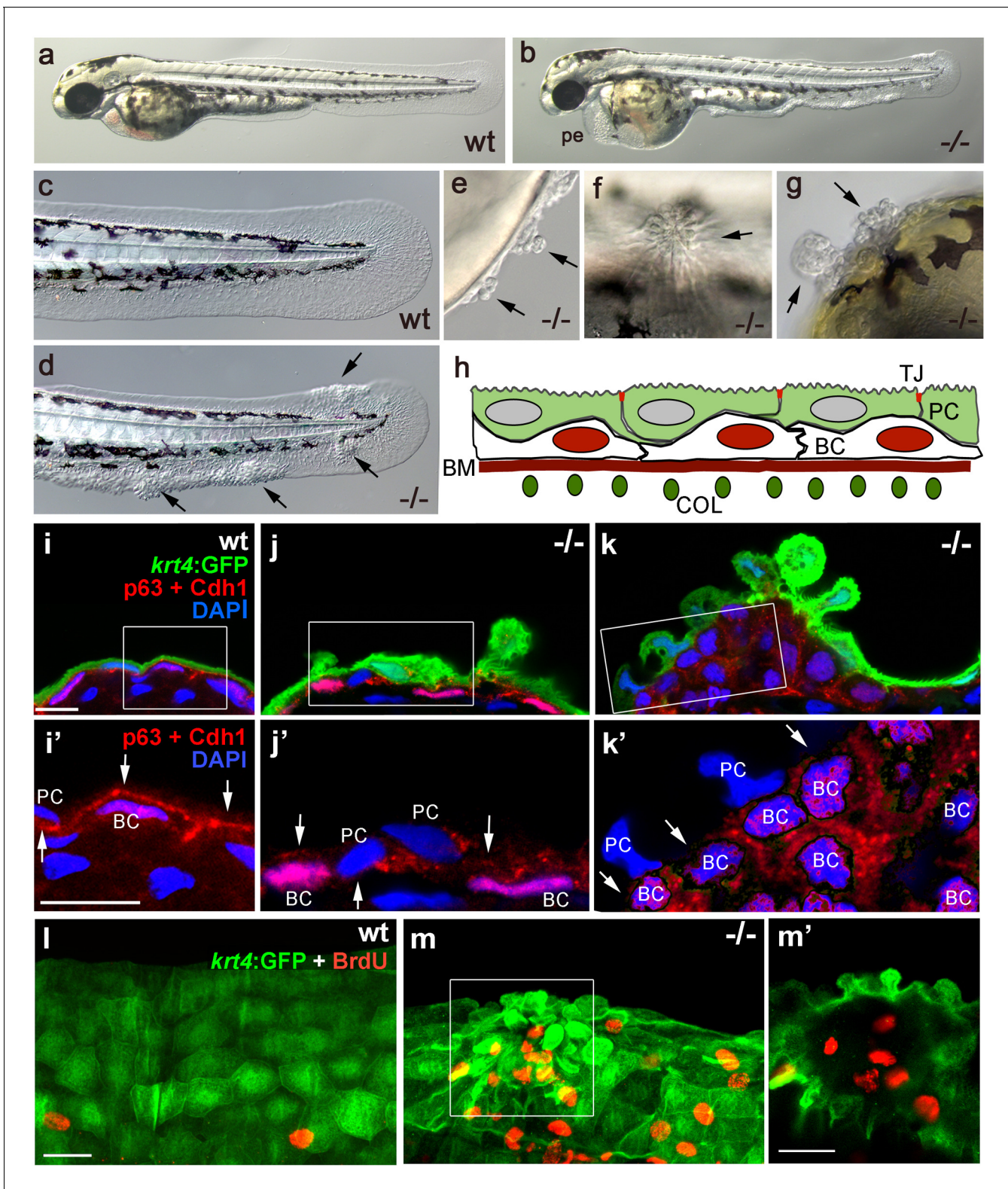


Figure 1. Epidermal aggregates in psoriasis mutants display hyperplasia. (a–g) Live images of wt siblings (a,c) and psoriasis mutants (b,d–g); psoriasis mutants develop pericardial edema (pe) and epidermal aggregates on the medium fin fold (b, d), on the yolk sac (e), on the flank (f) (all at 54 hpf), and on the head (g; 72 hpf). (h) Schematic of embryonic skin. Peridermal cells (PC, green) with apical tight junctions (TJ, red) are located above p63 basal keratinocytes (BC, red nuclei). The basement membrane (BM, red) separates the basal epidermal layer from the dermis containing collagen fibers (COL, green). (i–k) IF of periderm-specific GFP (green), Cdh1 (red), and p63 (red) on transverse sections through 48 hpf *Tg(krt4:GFP)* wt and psoriasis mutant embryos. (i'–k') Higher magnification views of the periderm in wt and -/- embryos. (l–m) krt4:GFP (green) and BrdU (red) staining in wt and -/- embryos, respectively. (l'–m') Higher magnification views of the -/- embryo showing hyperplasia. *Figure 1 continued on next page*

Figure 1 continued

embryos, counterstained with DAPI (blue). (i'–k') show magnified views of regions framed in (i–k), without the green channel. In wt, the epidermis is bi-layered, with flat cells (i) and Cdh1 is localized at cell borders between peridermal and basal cells (i'; arrows). In an early-stage aggregate of the mutant, peridermal cells have rounded up (j), and Cdh1 levels are reduced at cell borders (j',k'; arrows). An advanced aggregate (k) contains multi-layered basal epidermal cells (k'). Scale bar: 10 μm . (l,m) Whole mount IF of incorporated BrdU (red) and periderm-specific GFP (green) in 54 hpf *Tg(krt4:GFP)* wt sibling (l) and *psoriasis* mutant (m), showing elevated numbers of BrdU-positive non-peridermal cells in aggregates. (m) Maximum intensity projection of a confocal Z stack through aggregate; (m') single focal plane. Scale bars: 20 μm . Abbreviations: BC, basal cell; BM, basement membrane; COL, collagen fibers; PC, peridermal cell; pe, pericardial edema; wt, wild-type.

DOI: [10.7554/eLife.14277.003](https://doi.org/10.7554/eLife.14277.003)

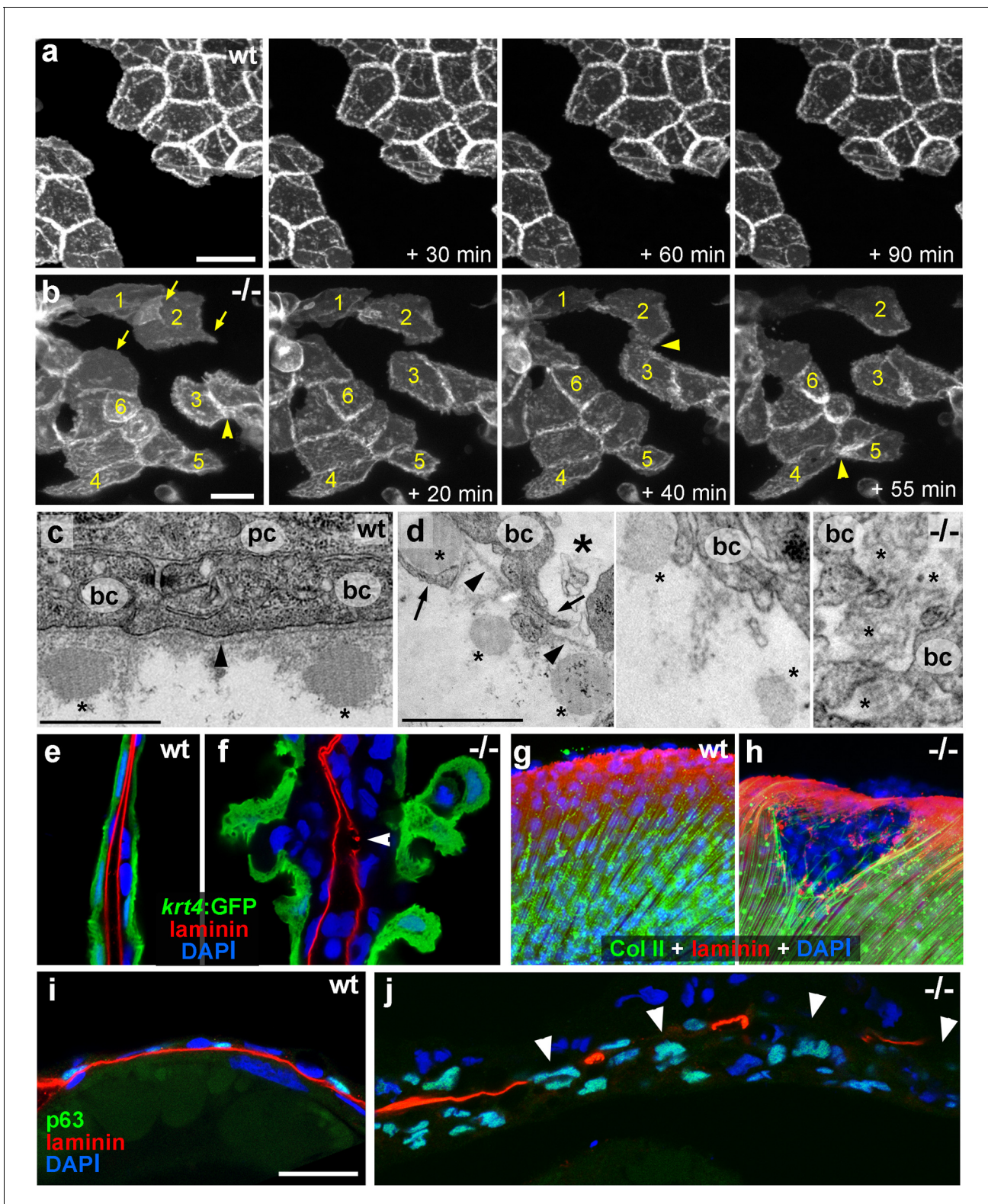


Figure 2. psoriasis keratinocytes display partial EMT and invasive behavior. (a,b) Stills from in vivo time-lapse recordings (**Videos 1** and **2**) of clones of membrane-bound GFP-labelled (*Tg(Ola.Actb:Hsa.hras-egfp)*) basal keratinocytes in a mosaic wt (a) or an *atp1b1a* morphant (b) embryo; 'n min' indicates elapsed time since the start of the recordings at 48 hpf (**Videos 1** and **2**). Wild-type cells form a rigid epithelium and maintain their shapes and relative positions (a), whereas *atp1b1a* morphant cells form cellular processes (arrows), dynamically dis- and re-associate (arrowheads) and eventually crawl on top of each other (cell 1; b, first panel). Cell 1 moves out of the focal plane after 60 min, cell 6 changes its shape from roundish to

Figure 2 continued on next page

Figure 2 continued

more hexagonal and vice versa. Scale bars: 20 μm . (c,d) Transverse TEM sections through median fin fold, at 58 hpf. In wt (c), an intact basement membrane (BM; black arrowhead) separates the compact layer of basal cells from the underlying dermis, which contains actinotrichia (small asterisks). The *psoriasis* mutant (d) displays large intercellular gaps (large asterisk) between basal cells, cellular protrusions (arrows) of basal cells, a discontinued BM (arrowheads to remaining BM), direct contacts between epidermal cells, and disassembling dermal actinotrichia (small asterisks) that lose their regular shape and striated pattern. bc: basal cells; pc: peridermal cell. Scale bars: 1 μm . (e,f) Laminin and peridermal-specific GFP double IF, counterstained with DAPI, at 58 hpf. Transverse sections through the fin fold of *Tg(krt4:GFP)* transgenics reveal basement membrane fragmentation (arrowhead) below an epidermal aggregate in the mutant (f). (g,h) Laminin and type II collagen double IF, counterstained with DAPI at 58 hpf; view of fin folds of whole mounts, showing basement membrane fragmentation and actinotrichia disassembly in the mutant (h). (i,j) Laminin and p63 double IF, counterstained with DAPI at 58 hpf; transverse section through the yolk sac. Arrowheads in (j) point to holes in the basement membrane of the mutant. Note the presence of p63 keratinocytes below the basement membrane in the dermal space. Scale bar: 20 μm .

DOI: [10.7554/eLife.14277.004](https://doi.org/10.7554/eLife.14277.004)

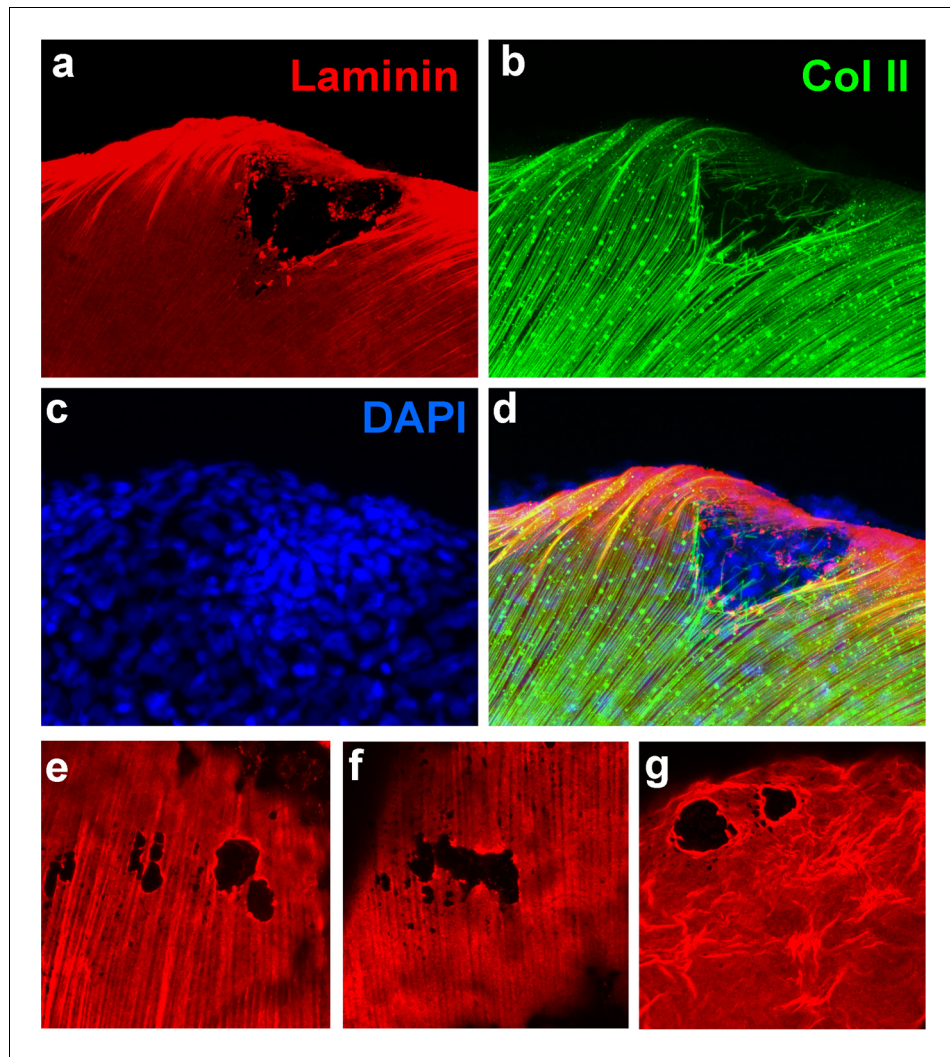


Figure 2—figure supplement 1. *psoriasis* mutants display local degradations of the skin basement membrane and of underlying collagenous actinotrichia of the dermis. (a-d) IF of laminin (red; a) and type II collagen (green; b) in a whole mount 58 hpf *psoriasis* mutant fin fold, counterstained with DAPI (blue; c). The basement membrane is disintegrated (a) and actinotrichia (b) are disassembled below an epidermal aggregate (d; merged channels). (e–g) IFs of laminin (red) show examples of holes in the basement membrane in different 58 hpf *psoriasis* mutants. DOI: [10.7554/eLife.14277.005](https://doi.org/10.7554/eLife.14277.005)

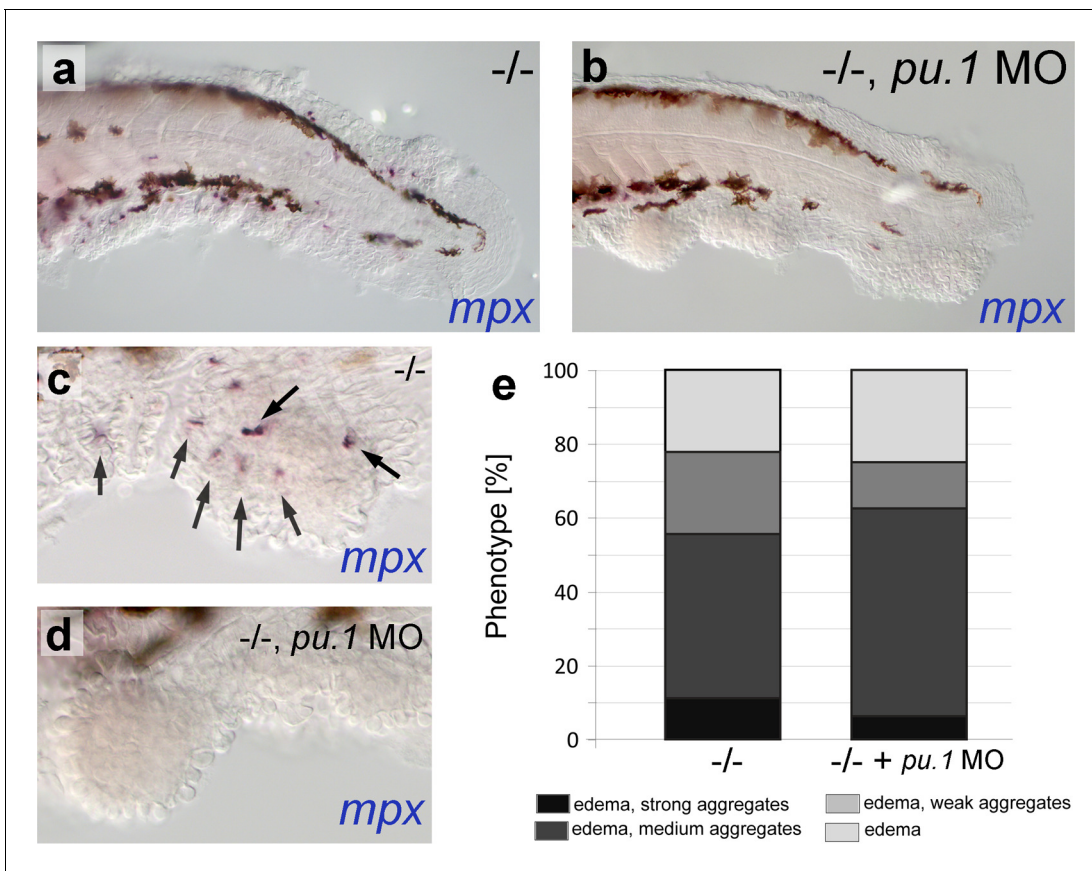


Figure 2—figure supplement 2. *psoriasis* mutants display skin inflammation, which does not contribute to the formation of epidermal aggregates. (a–d) WISH of *mpx* labeling neutrophils in 54 hpf *psoriasis* $-/-$ and *psoriasis* $-/-$; *mpx* MO embryos. *mpx*-positive neutrophils (arrows) have migrated into epidermal aggregates in the *psoriasis* $-/-$ embryo (a,c). No reduction of epidermal aggregate formation and no *mpx*-positive neutrophils are observed in *psoriasis* mutants, in which the myeloid lineage has been ablated by *pu.1* MO injection (b, d). (e) Quantification of phenotypes of *psoriasis* mutants injected with *pu.1* MO and un-injected controls. n = 16–18.

DOI: [10.7554/eLife.14277.006](https://doi.org/10.7554/eLife.14277.006)

The following source data is available for figure 2:

Figure supplement 2—Source data 1. Source data for **Figure 2—figure supplement 2e**.

DOI: [10.7554/eLife.14277.007](https://doi.org/10.7554/eLife.14277.007)

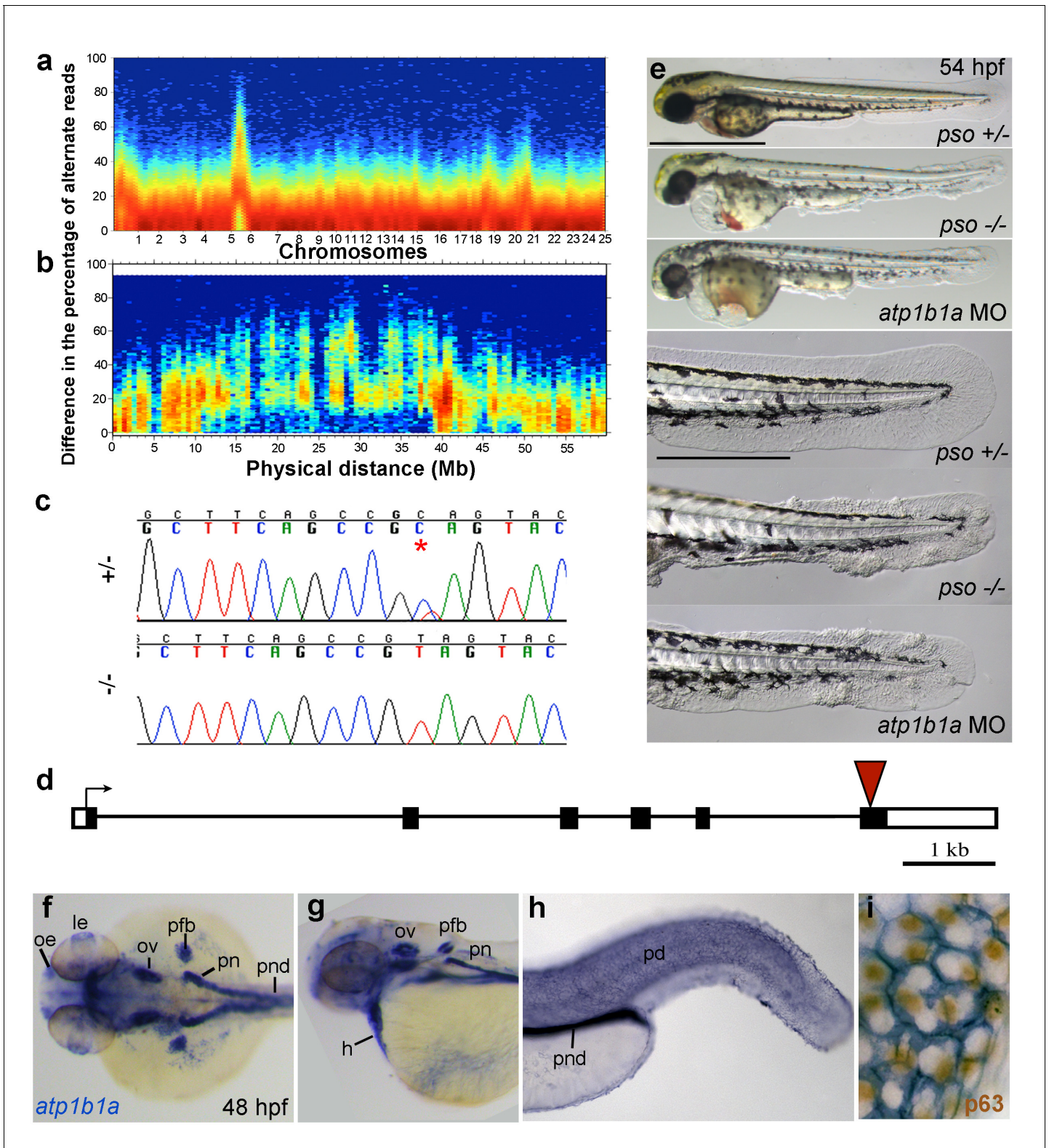


Figure 3. The psoriasis phenotype is caused by a loss-of-function mutation in *atp1b1a*, which is expressed in multiple epithelia, but not in basal keratinocytes. (a-d) Exome sequencing links the psoriasis mutation to LG6 and identifies a C to T transition in *atp1b1a*. (a,b) Heat maps showing the density of variant loci over the whole genome (a) and on chromosome 6 (b). The Y-axis shows the absolute value of the difference in the percentage of DNA harboring the variation between the pool of affected offspring and the pool of their parents. Most of the genome shows a difference close to 0%, indicating that the parental DNA segregated randomly in the affected offspring. Only one peak on chromosome 6 shows low density at a difference of

Figure 3 continued on next page

Figure 3 continued

0%, but high density at between 25% and 50% difference, which is expected at the linked locus under the assumption of a recessive mode of inheritance. (c) Chromatographs of Sanger sequencing of sibling and mutant DNA showing the *psoriasis* mutation (*). (d) Schematic representation of the *atp1b1a* locus. Red arrowhead indicates the position of the mutation. (e) Live images of 54 hpf wt siblings, *psoriasis* mutants, and *atp1b1a* morphants. MO-based knockdown of *atp1b1a* in wt embryos phenocopies both the pericardial edema and epidermal aggregates. Scale bars: 500 μm ; 250 μm (magnifications). (f–i) WISH detects *atp1b1a* RNA (blue) in heart and multiple epithelia of 48 hpf wt embryos, including the pronephric duct and the periderm but not in the basal keratinocytes (f–h), as seen at higher magnification after counterstaining of nuclei of basal keratinocytes for p63 protein (i). The *atp1b1a* RNA signal is not detected around p63 nuclei, but is detected in hexagonal peridermal cells with p63⁻ nuclei. Abbreviations: h, heart; le, lense; oe, olfactory epithelium; ov, otic vesicle; pd, periderm; pfb, pectoral fin bud; pn, pronephros; pnd, pronephric duct.

DOI: [10.7554/eLife.14277.010](https://doi.org/10.7554/eLife.14277.010)

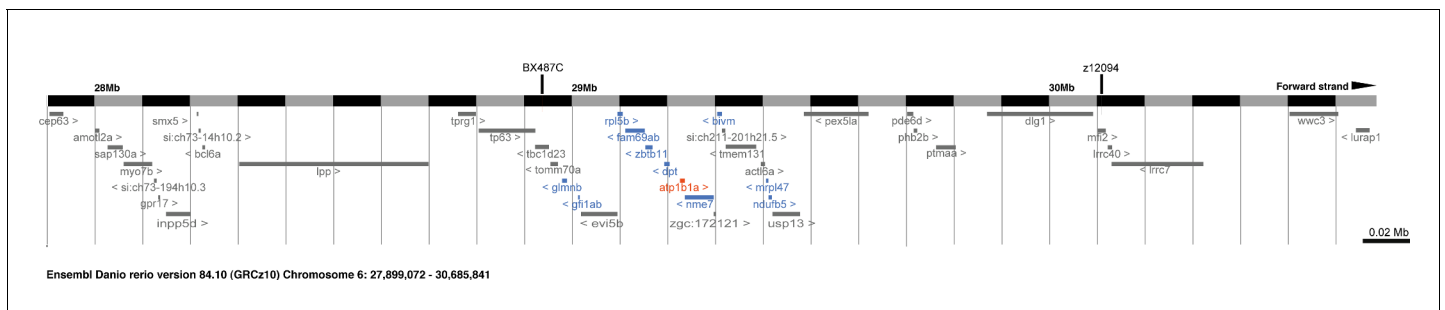


Figure 3—figure supplement 1. Schematic of the genomic region between 27,899,072–30,685,841 on Chromosome 6 of Ensembl *Danio rerio* version 84.10 (GRCz10). Merged Havana/Ensemble annotated genes are indicated. The interval between the two simple sequence length polymorphism (SSLP) markers BX487C and z12094, to which *atp1b1a* had been meiotically mapped by **Webb et al., 2008**, is indicated by black bars. Exons of genes indicated in grey and red have been exclusively sequenced in this study, and a nonsense mutation has been identified in *atp1b1a* (red). Genes indicated in blue have been sequenced in this study as well as by **Webb et al., 2008** without identification of mutagenic lesions.

DOI: [10.7554/eLife.14277.011](https://doi.org/10.7554/eLife.14277.011)

The following source data is available for figure 3:

Figure supplement 1—Source data 1. List of annotated genes, in syntenic order, contained in the genomic 2.76 Mb region shown in **Figure 3—figure supplement 1**, together with their chromosomal location, and their sequencing status.

DOI: [10.7554/eLife.14277.012](https://doi.org/10.7554/eLife.14277.012)

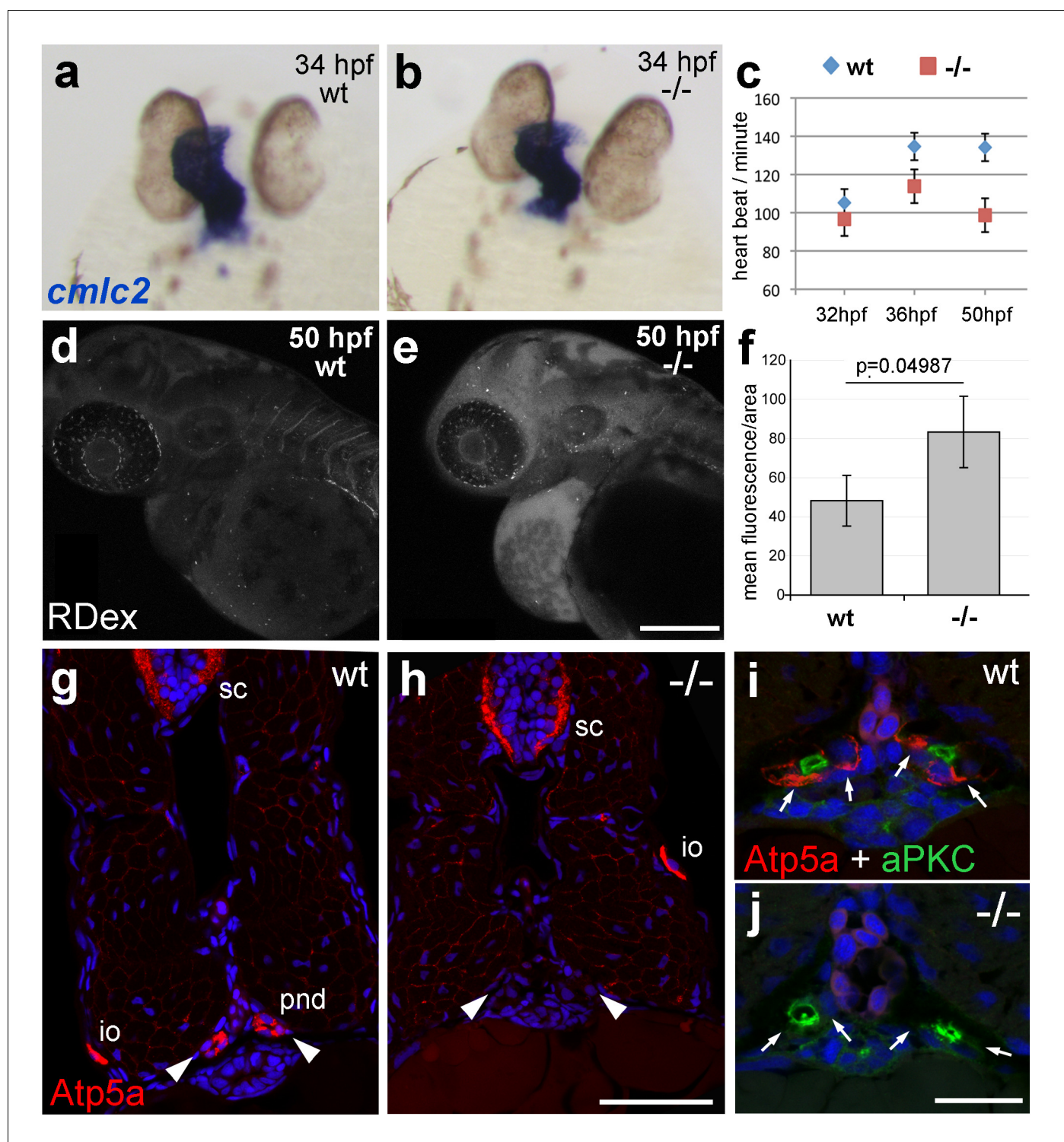


Figure 4. *atp1b1a* is required for proper heart and pronephric function. (a, b) WISH of *cmlc2* in 34 hpf embryos reveals normal heart tube elongation in *psoriasis* mutants. (c) *psoriasis* mutants exhibit a reduction of the heart beat. n = 12 (mutants), 24 (siblings). p values: 32 hpf: 3.8E-04, 36 hpf: 6.8E-07, 50 hpf: 1.2E-11. (d–f) *psoriasis* mutants show compromised clearance / excretion of rhodamine-dextrane injected into the cardinal vein at 34 hpf; confocal images of live embryos of wt sibling (e) and mutant (f) embryos at 50 hpf; RDex, rhodamine-dextrane; scale bar: 200 μ m. (f) Quantification of mean fluorescence intensity of a defined area in confocal images, determined with ImageJ software; n = 3 for each condition. Error bars represent standard deviations. (g–j) IF of Atp5a (red) and aPKC (green), counterstained with DAPI (blue), on transverse sections of 54 hpf wt (g,i) and *psoriasis* mutant (h,j) embryos. Atp5a signal is absent from the pronephric duct (pnd, arrowheads) but not from ionocytes (io) or spinal cord (sc) in *psoriasis* mutants (g,h).

Figure 4 continued on next page

Figure 4 continued

The apical marker aPKC is still present in the pronephric duct cells of *psoriasis* mutants, outlining the lumen of the ducts, whereas Atp5a is missing from the basolateral site (arrows; i,j).

DOI: [10.7554/eLife.14277.013](https://doi.org/10.7554/eLife.14277.013)

The following source data is available for figure 4:

Source data 1. Source data for **Figure 4.**

DOI: [10.7554/eLife.14277.014](https://doi.org/10.7554/eLife.14277.014)

Figure 5 continued

not in the mutant raised in isotonic E3 (d). IF of BrdU incorporation (white) in 72 hpf wt or *atp1b1a* morphant tail fins (e–h) reveals excessive cell proliferation in the fin fold of the morphant embryo (f) raised in hypotonic E3 but not in the morphant embryo (h) raised in isotonic E3. (i) Quantification of embryos as shown in (a–d), obtained from incross of two *psoriasis* *-/-* parents. n = 86–122. (j) Representative gel with PCR products subjected to *MwoI* restriction digest to genotype embryos raised in isotonic medium. All mutants raised in isotonic medium and shown as representative examples in this and the following figures had been positively genotyped. (k) Quantification of embryos as shown in (e–h), scored is the number of BrdU-positive cells in a given area of the median fin fold. n = 3–7 per condition. Error bars represent standard deviation. p values are as follows: a: 0.0416, b: 0.9139, c: 0.8956, d: 0.0017. (l–n) Live images of 56 hpf wt embryos (l,l'), *psoriasis* mutant embryos (m,m'), and wt embryos treated with 3mM ouabain (n,n') starting from 33 hpf. Blockage of Na,K-ATPase pump function by ouabain results in pericardial edema (pe) as in *psoriasis* mutants (n = 122/125; compare n to m), but not in epidermal aggregates (n = 0/125; compare n' to m').

DOI: [10.7554/eLife.14277.015](https://doi.org/10.7554/eLife.14277.015)

The following source data is available for figure 5:

Source data 1. Source data for **Figure 5**.

DOI: [10.7554/eLife.14277.016](https://doi.org/10.7554/eLife.14277.016)

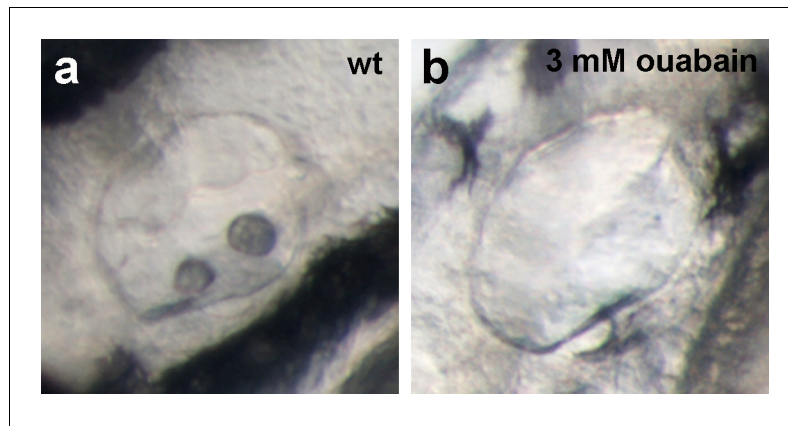


Figure 5—figure supplement 1. Live images of the otic vesicles of 48 hpf embryos show two otoliths in a untreated wt embryo (a) whereas in an embryo treated with 3 mM ouabain starting from 10 hpf, otoliths have failed to form (b; n = 76/99) or are much smaller (not shown; n = 23/99).

DOI: [10.7554/eLife.14277.017](https://doi.org/10.7554/eLife.14277.017)

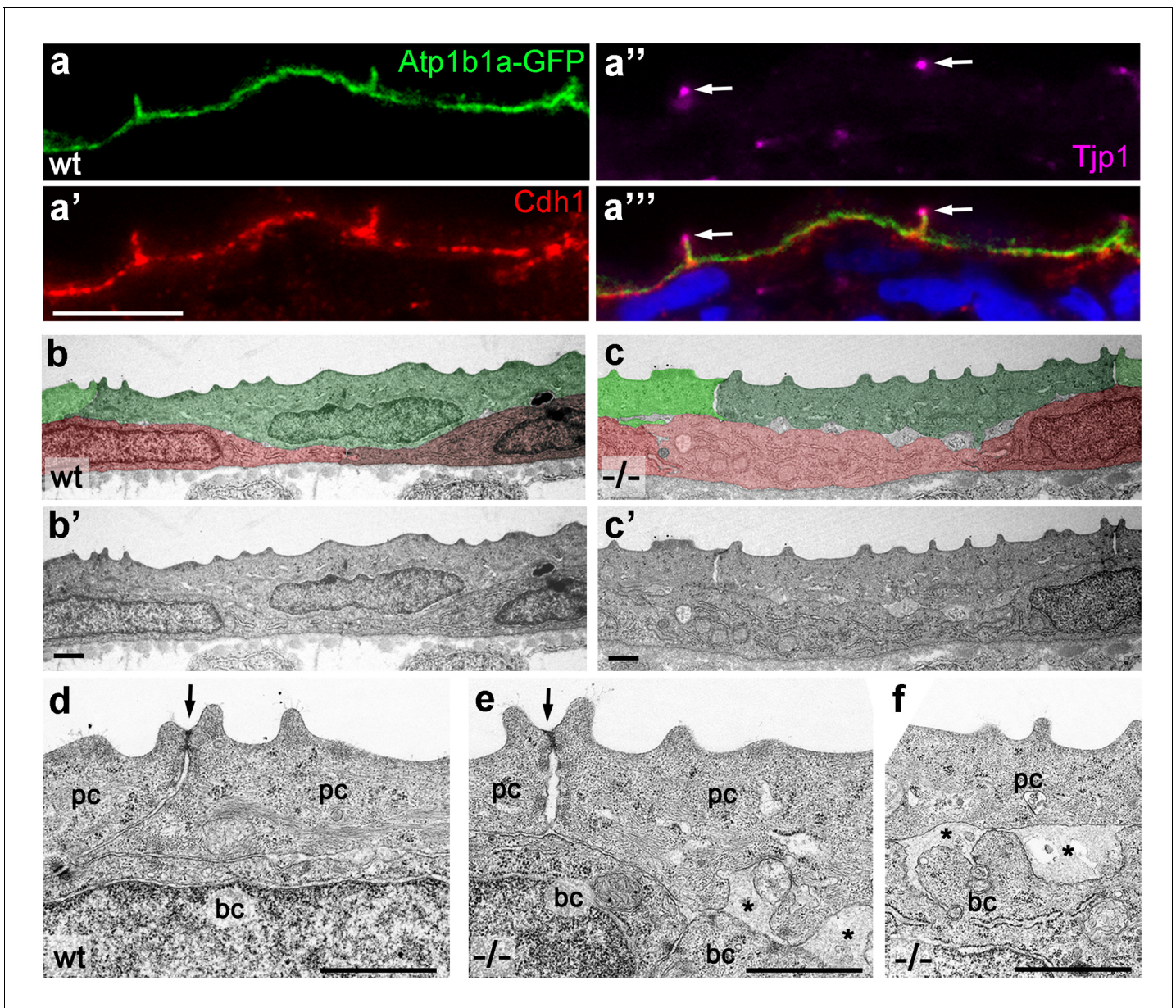


Figure 6. Atp1b1a is required for epidermal cell adhesion. (a) IF of GFP (a, green), Cdh1 (a', red) and tight junction marker Tjp1 (a'', magenta) on a transverse section of the epidermis of a 48 hpf wt embryo expressing peridermal-specific *krt4:atp1b1a-gfp*, counterstained with DAPI (blue; a''' with merged channels). Atp1b1a and Cdh1 are co-localized on the basolateral side of peridermal cells, but are excluded from tight junctions and the apical side of these cells. (b–f). Transverse TEM sections through the medium fin fold of wt and *psoriasis* mutant embryos raised in isotonic conditions, at 58 hpf. In the mutant epidermis (c,c'), aberrant gaps between peridermal cells (false-colored in green) and underlying keratinocytes (false-colored in red) are apparent when compared to the wt epidermis (b,b'). (d–f) Higher magnifications reveal tight junctions (indicated by arrows) of unaltered morphology in the mutant (e) compared to a wt sibling (d), but less organized lateral regions between peridermal cells (e), and large gaps (*) between peridermal and basal cells (e,f) in the mutant. bc, basal cell; pc, peridermal cell. Scale bars: 1 μm.

DOI: [10.7554/eLife.14277.018](https://doi.org/10.7554/eLife.14277.018)

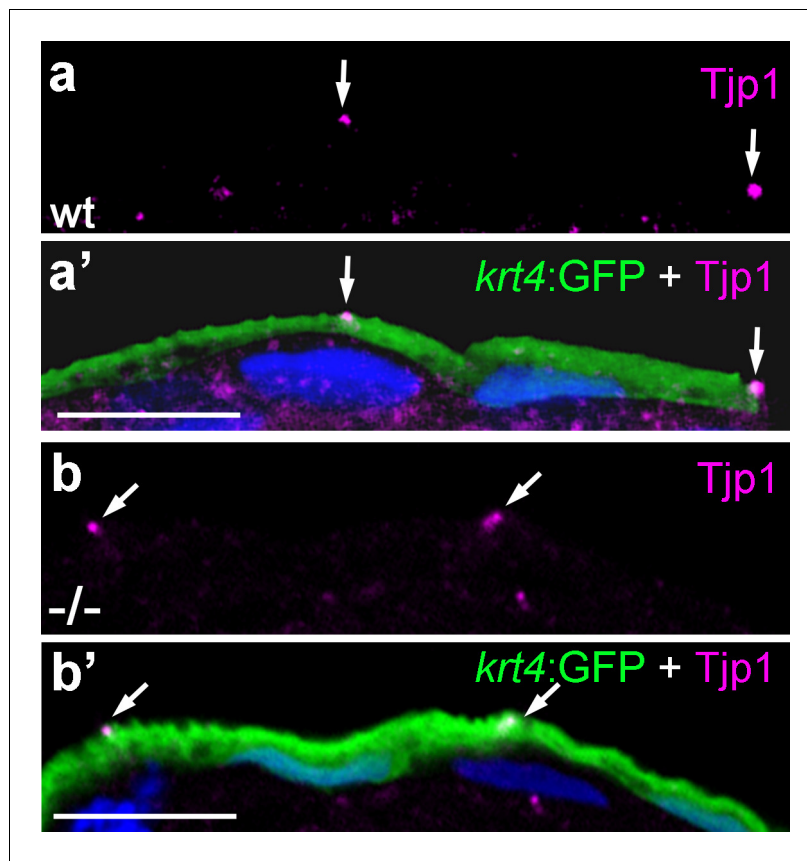


Figure 6—figure supplement 1. Localization of the tight junction protein Tjp1 is unaltered in *psoriasis* mutants. IF of Tjp1 (a,b; magenta) and periderm-specific GFP (a',b'; green; counterstained with DAPI in blue; merged channels); transverse section through epidermis of wt (a,a') and *psoriasis* mutant (b,b') embryos carrying *Tg(krt4:GFP)* transgene; 48 hpf., Tjp1 (arrowed) shows unaltered apical localization in peridermal cells of mutant. Scale bar: 10 μ m.

DOI: [10.7554/eLife.14277.019](https://doi.org/10.7554/eLife.14277.019)

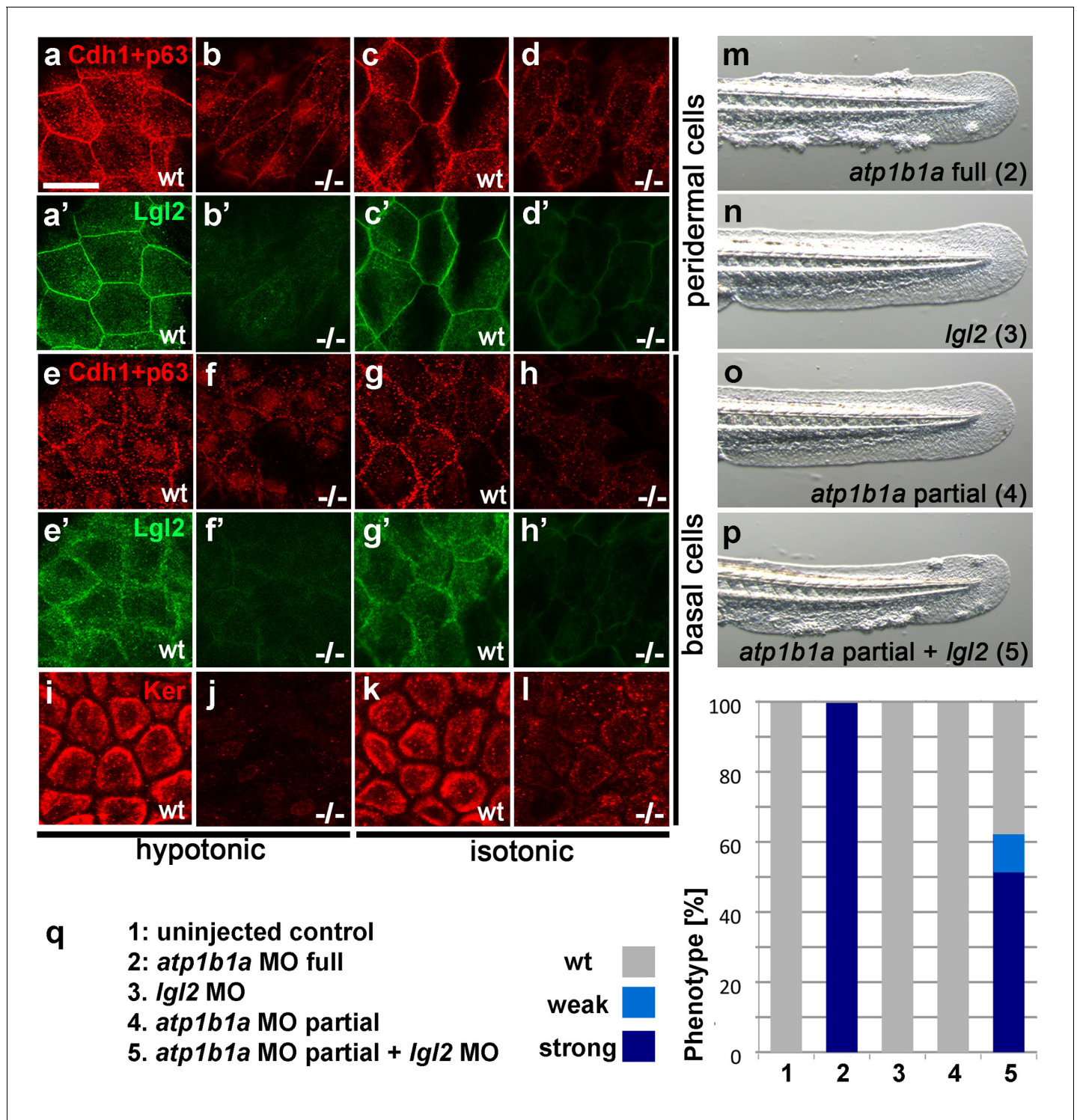


Figure 7. Atp1b1a is required for epidermal integrity and polarity. (a–h). Whole mount IFs of Cdh1 (red) and Lgl2 (green) in 54 hpf embryos raised in hypotonic (a,b,e,f) and isotonic (c,d,g,h) conditions. In mutants, localization of Cdh1 (b, d, f, and h; compare to wt a, c, e, g) and Lgl2 (b', d', f', and h'; compare to wt a', c', e', g') is compromised in both peridermal cells (a–d) and basal cells (e–h). Images show regions of the trunk epidermis not yet affected by aggregate formation. (i–l). Whole mount IFs of cytokeratin (red) in 84 hpf embryos show a reduction of basally localized cytokeratin in mutants raised in hypotonic (j) and isotonic (l) conditions. Images show regions of the trunk epidermis above the yolk sac extension. (m–p). Live images of the tail fins of 54 hpf embryos either with full MO knockdown of *atp1b1a* (m) or with partial MO knockdown of *lgl2* (n), of *atp1b1a* (o), or of both (p).
Figure 7 continued on next page

Figure 7 continued

(q) Quantification of the phenotypes of 54 hpf embryos in synergistic enhancement studies; n = 31–88. Similar results were obtained in two additional independent experiments.

DOI: [10.7554/eLife.14277.020](https://doi.org/10.7554/eLife.14277.020)

The following source data is available for figure 7:

Source data 1. Source data for **Figure 7q**.

DOI: [10.7554/eLife.14277.021](https://doi.org/10.7554/eLife.14277.021)

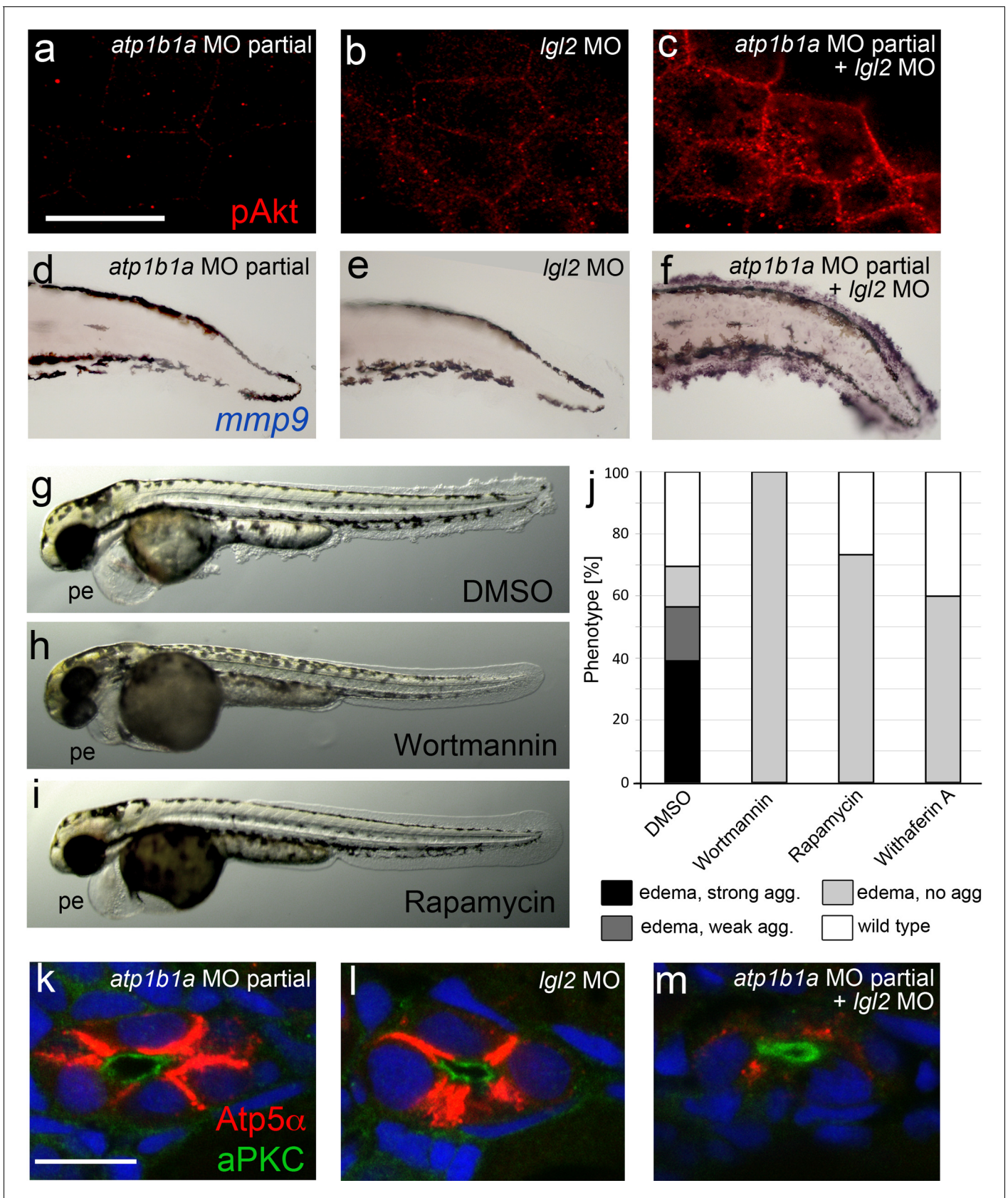


Figure 7—figure supplement 1. *atp1b1a* and *Igl2* interact genetically to enhance edema formation and AKT phosphorylation and *mmp9* expression in Figure 7—figure supplement 1 continued on next page

Figure 7—figure supplement 1 continued

basal keratinocytes of embryos raised in hypotonic medium. (a–c) pAKT IF, at 54 hpf, revealing low pAKT levels in embryos injected with low amounts of *atp1b1a* MO (a) or with *Igl2* MO (b), but strongly increased levels in a double-injected embryo (c). For comparison with pAKT levels in wild-type and *psoriasis* mutants (full loss of Atp1b1a activity), see **Figure 8f,g**. (d–f). *mmp9* WISH, at 54 hpf, revealing low *mmp9* expression in embryos injected with low amounts of *atp1b1a* MO (d) or with *Igl2* MO (e), but strongly increased levels in double-injected embryo (f). For comparison with *mmp9* expression levels in wild-type and *psoriasis* mutant, see **Figure 9j,j'**. (g–j). Embryos co-injected with sub-phenotypic amounts of *atp1b1a* MO and *Igl2* MO display epidermal aggregates in conjunction with pericardial edema. Treatment with the PI3K inhibitor Wortmannin, the mTORC1 inhibitor Rapamycin or the NFκB inhibitor Withaferin A, starting at 34 hpf, leads to a complete loss of epidermal aggregates, whereas edema persists. (g–i) Representative live images of DMSO-treated controls (g), and of Wortmannin-treated (h) and Rapamycin-treated (i) embryos, at 54 hpf; pe, pericardial edema. (j) Quantification of the phenotypes of control, Wortmannin-, Rapamycin- or Withaferin A-treated embryos as shown in (g–i), at 54 hpf. For classification of phenotypic strengths, see **Figure 9a–d**. (k–m). IF of Atp5a (red) and aPKC (green), counterstained with DAPI (blue), on transverse sections at 54 hpf, revealing high amounts of Na,K-ATPase α -subunits in the basolateral membrane domains of pronephric duct epithelial cells in embryos injected with low amounts of *atp1b1a* MO (k) or with *Igl2* MO (l), but strongly decreased levels in double-injected embryo (m). Scale bar: 10 μ m.

DOI: [10.7554/eLife.14277.022](https://doi.org/10.7554/eLife.14277.022)

The following source data is available for figure 7:

Figure supplement 1—Source data 1. Source data for **Figure 7—figure supplement 1j**.

DOI: [10.7554/eLife.14277.023](https://doi.org/10.7554/eLife.14277.023)

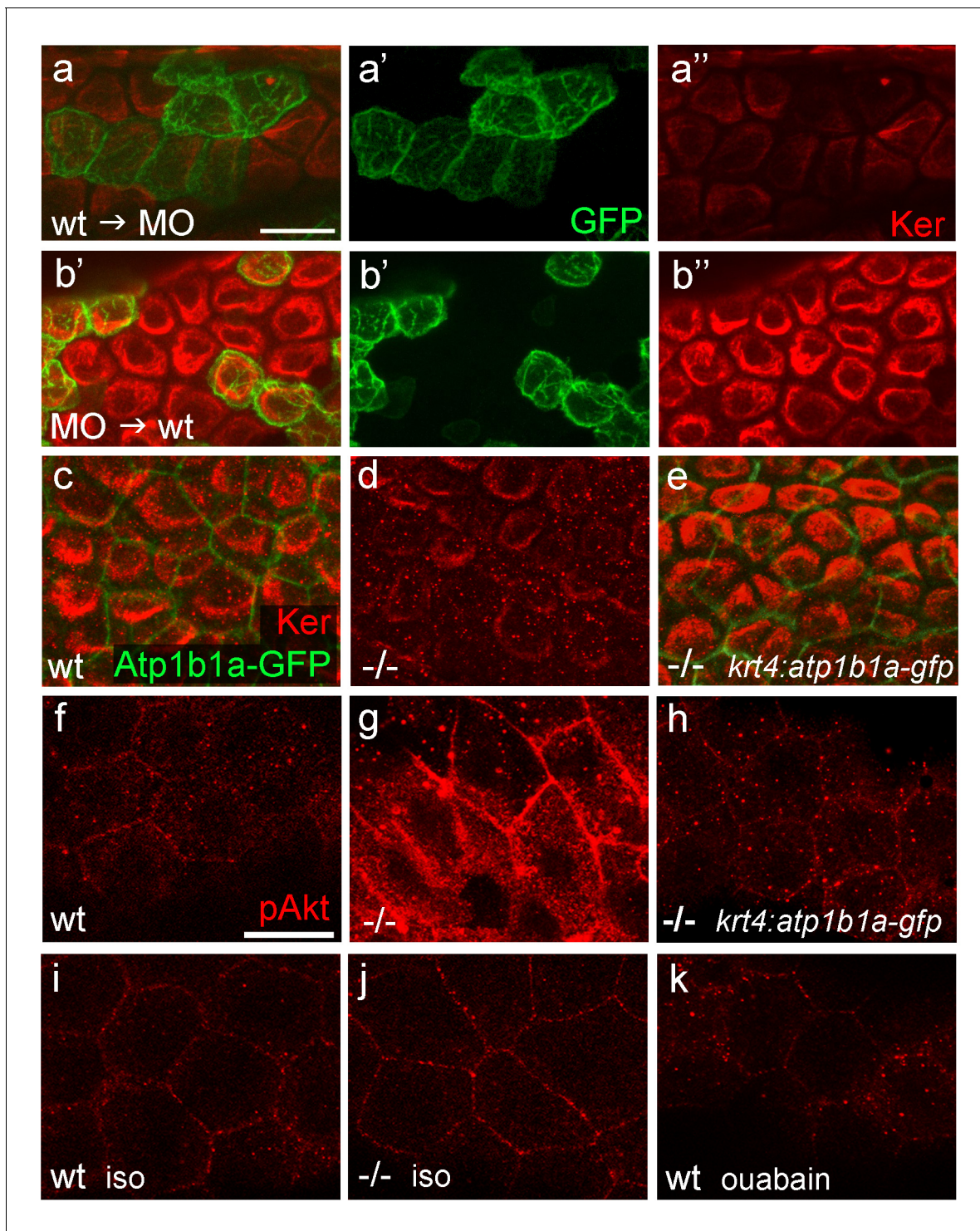


Figure 8. *atp1b1a* is required in peridermal cells to establish epithelial organization of basal keratinocytes, and to suppress hypotonicity-induced upregulation of pAKT levels in basal keratinocytes. (a–b) IF of cytokeratins (Ker; red) and GFP (green) in 84 hpf chimeric embryos raised in isotonic conditions. Wild-type (wt) basal keratinocytes expressing *Tg(Ola.Actb:Hsa.hras-egfp)*-encoded membrane-tagged GFP transplanted into *atp1b1a* morphant hosts display reduced cytokeratin localization similar to that of host cells (a), whereas the cytokeratin distribution of morphant donor cells (green) in wt hosts is indistinguishable from that in neighboring wt cells (b). Images show regions of the trunk epidermis above the yolk sac extension. (c–e). Maximum intensity projections of confocal images of IF of cytokeratin (red) and periderm-specific *Atp1b1a*-GFP (green) in 84 hpf embryos obtained from an in-cross of *psoriasis +/-*; *Tg(krt4:atp1b1a-gfp)* parents, raised in isotonic conditions. Embryos were genotyped after imaging. Cytokeratin localization in basal keratinocytes is distorted in non-transgenic *psoriasis*^{-/-} embryos (d; compare to wt in c), but restored in *psoriasis*^{-/-}; *Tg* Figure 8 continued on next page

Figure 8 continued

(*krt4:atp1b1a-gfp*) embryos (e). Images show regions of the trunk epidermis above the yolk sac extension. (f–k) pAKT IF (red) in 54 hpf embryos. pAkt is upregulated in *psoriasis* mutants raised in hypotonic (g) but not in isotonic (j) medium, compared to wt siblings (f, i). pAkt levels are ameliorated in *psoriasis*^{-/-}; *Tg(krt4:atp1b1a-gfp)* embryos kept in hypotonic medium (h). pAkt is not upregulated in wt embryos incubated in hypotonic medium after addition of 3 mM ouabain, starting from 33 hpf (k). Images show regions of the trunk epidermis not yet affected by aggregate formation. Abbreviation: iso, isotonic medium (E3 250 mM mannitol).

DOI: [10.7554/eLife.14277.024](https://doi.org/10.7554/eLife.14277.024)

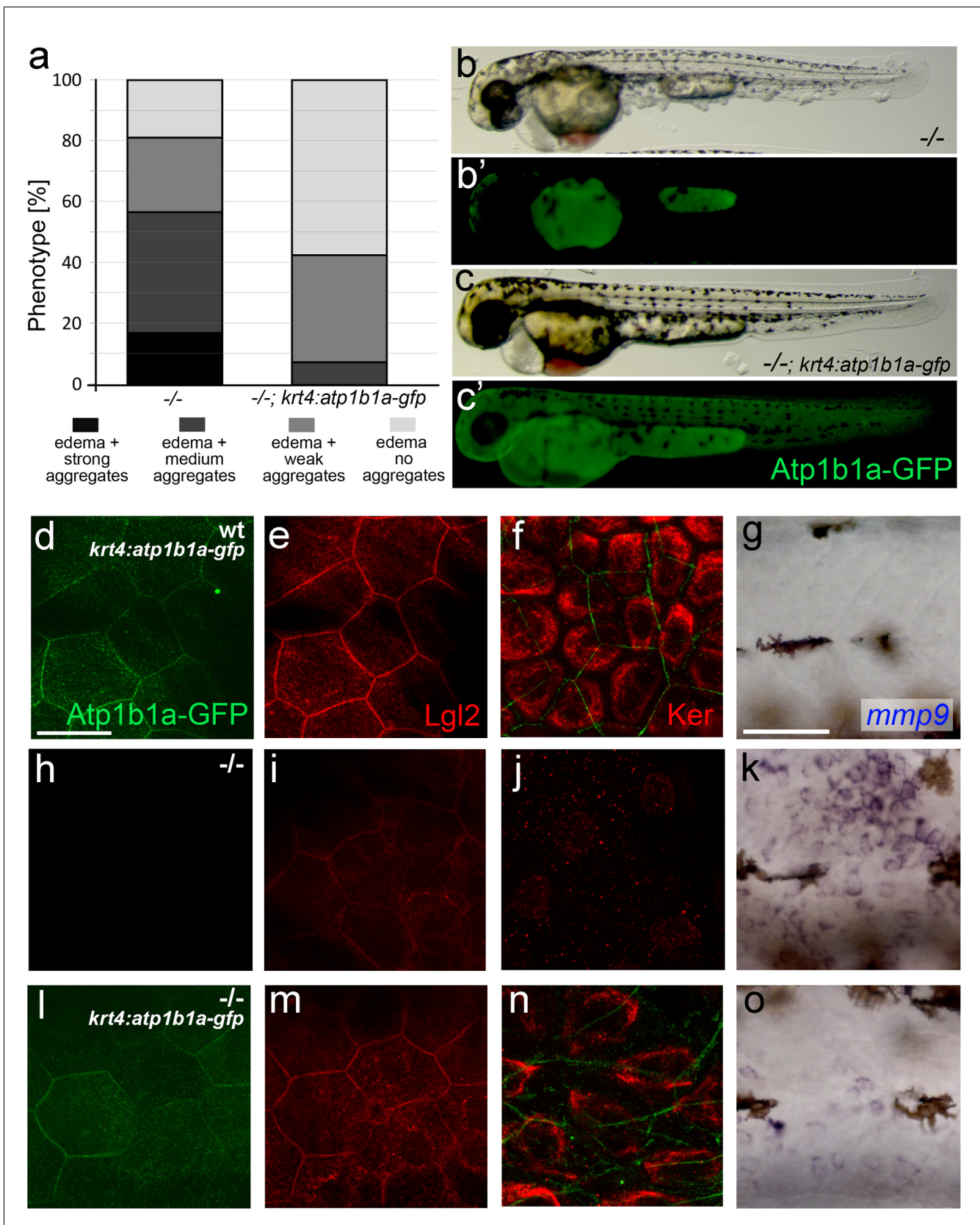


Figure 8—figure supplement 1. *Tg(krt4:atp1b1a-gfp)*-driven *atp1b1a* expression in the periderm of *psoriasis* mutants kept in hypotonic medium leads to a partial rescue of the polarity defects and malignant transformation in basal keratinocytes. (a) Quantification of phenotypes of non-transgenic Figure 8—figure supplement 1 continued on next page

Figure 8—figure supplement 1 continued

psoriasis mutants and *psoriasis* mutants carrying the *krt4:atp1b1a-gfp* transgene, raised in hypotonic E3, at 54 hpf. For classification of phenotypic strengths, see **Figure 9a–d**. (**b–c**) Representative live images of a *psoriasis* mutant lacking the transgene (no peridermal GFP; **b'**), which has pericardial edema and epidermal aggregates (**b**), and a *psoriasis* mutant expressing the transgene (peridermal GFP; **c'**), which has pericardial edema but no epidermal aggregates (**c**). (**d–o**) IF of GFP (transgene-encoded Atp1b1a-GFP) in periderm (**d**; green; **d,h,l**; 54 hpf), Lgl2 in periderm (**e**; red; **e,i,m**; 54 hpf) and cytokeratin in basal keratinocytes (**f**; red; **f,j,n**; 84 hpf), and WISH of *mmp9* transcripts in basal keratinocytes (**g,k,o**; 54 hpf) of transgenic wt siblings (**d–g**), non-transgenic *psoriasis* mutants (**h–k**) and *psoriasis* mutants carrying the *krt4:atp1b1a-gfp* transgene (**l–o**). Periderm-specific expression of *atp1b1a* in mutant embryos leads to a partial restoration of the polarity markers Lgl2 and cytokeratin, and to a reduction of the malignancy marker *mmp9*. However, obtained levels are still higher than in the wt sibling control. For the reduction of the malignancy marker pAKT, see **Figure 8f–h**. Scale bars: 20 μm (**d–f**, **h–j**, **l–n**) and 50 μm (**g**, **k**, **o**).

DOI: [10.7554/eLife.14277.025](https://doi.org/10.7554/eLife.14277.025)

The following source data is available for figure 8:

Figure supplement 1—Source data 1. Source data for **Figure 8—figure supplement 1a**.

DOI: [10.7554/eLife.14277.026](https://doi.org/10.7554/eLife.14277.026)

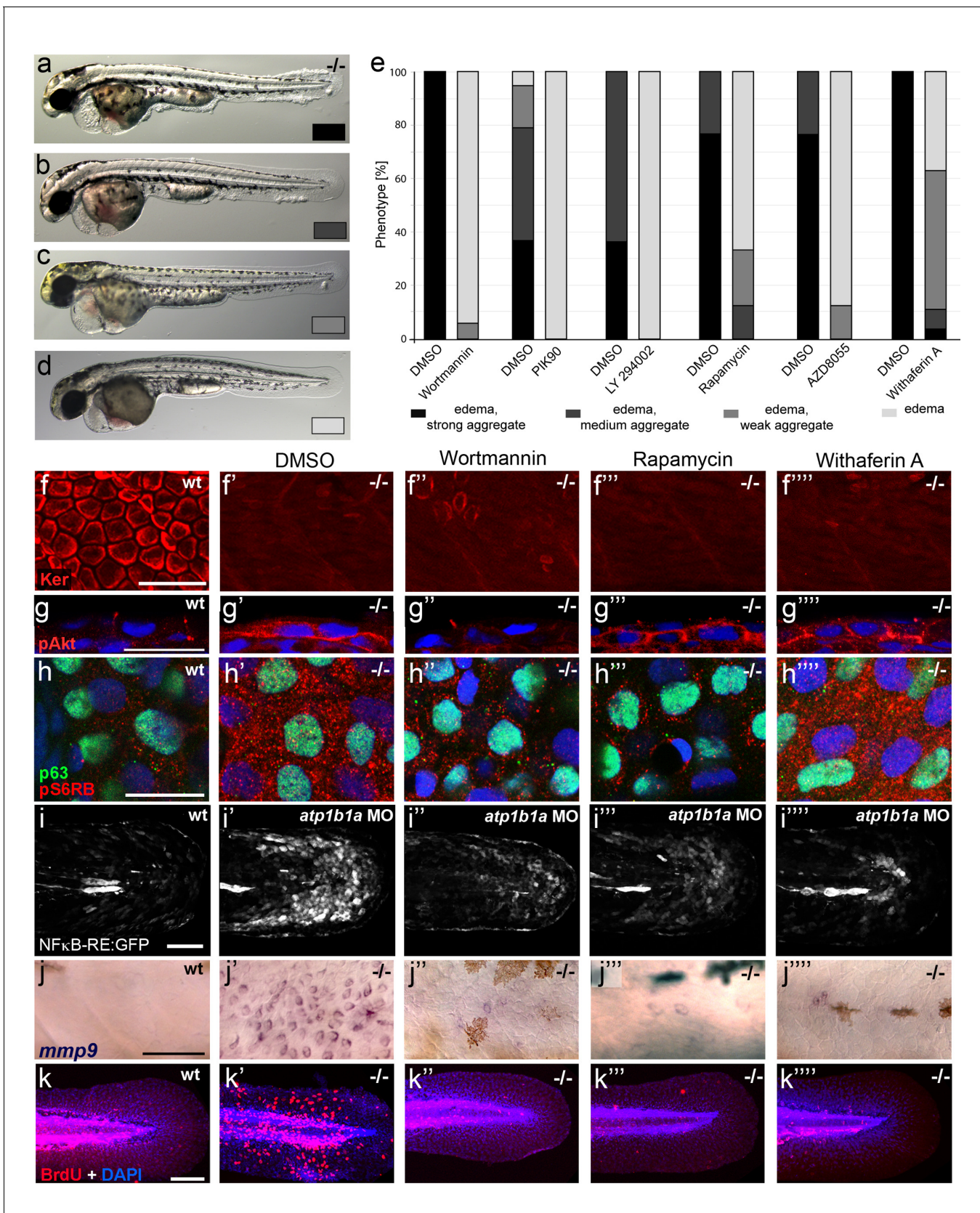


Figure 9. Hyperplasia and transcriptional upregulation of *mmp9* in basal keratinocytes of *psoriasis* mutants is mediated via an aberrant activation of a linear PI3K-Akt-mTorC1-NFκB pathway. (a–e) Blockade of PI3K, mTorC1, and NFκB signaling rescues epidermal aggregate but not pericardial edema. Figure 9 continued on next page

Figure 9 continued

formation in *psoriasis* mutants. (a–d) Representative live images of phenotypic strength classes of *psoriasis* *-/-* embryos at 54 hpf, all with pericardial edema of comparable strengths, but strong (a), intermediate (b), weak (c), or no (d) epidermal aggregates. (e) Quantification of the phenotypes of *psoriasis* mutants incubated in E3 medium containing 1 μ M Wortmannin, 5 μ M PIK90, 25 μ M LY94002, 1.1 μ M Rapamycin, 30 μ M AZD8055, or 30 μ M Withaferin A compared to the corresponding DMSO controls (n = 16–30). Drugs were added at 34 hpf and embryos scored at 54 hpf. Similar results were obtained in at least two additional independent experiments. For representative live images, see **Figure 9—figure supplement 1. f–k**. A linear PI3K-Akt-mTORC1-NF κ B pathway mediates hyperplasia and upregulation of *mmp9* expression in basal keratinocytes. All embryos had been kept in (hypotonic) E3 medium, supplemented with the indicated drugs starting at 34 hpf. (f–f''') IF of cytokeratins (red) at 84 hpf. Distorted keratin localization in the *psoriasis* mutant (f', compare to wt (f)) is not restored by Wortmannin (f''), Rapamycin (f'''), or Withaferin A (f'''). Scale bar: 50 μ m. (g–g''') IF of pAkt (red), counterstained with DAPI (blue); transverse sections of 54 hpf *psoriasis* mutants raised in E3 medium. Elevated pAkt levels in the mutant (g', compared to the wt (g)) are lowered by Wortmannin (g''), but not by Rapamycin (g''') or Withaferin A (g'''). Scale bar: 20 μ m. (h–h''') IF of pS6RP and p63 of whole mounts, at 54 hpf. Elevated pS6RP levels in mutant (h', compared to wt (h)) are alleviated by Wortmannin (h''), PIK90 (not shown) and Rapamycin (h'''), but not by Withaferin A (h'''). Scale bar: 20 μ m. (i–i''') Confocal images of GFP fluorescence in the tail fin of a live 48 hpf wt embryo (i) and an *atp1b1a* morphant (i'), both carrying the *Tg(NF κ B-RE:eGFP)* transgene. The *atp1b1a* morphant shows strong upregulation of NF κ B activity in keratinocytes, which is restored by treatment with Wortmannin (i''), Rapamycin (i'''), and Withaferin A (i'''). Scale bar: 100 μ m. For quantification, see **Figure 9—figure supplement 2. (j–j''')** *mmp9* WISH at 54 hpf. Elevated *mmp9* expression in the mutant epidermis (j', compare to wt (j)) is downregulated by Wortmannin (j''), Rapamycin (j'''), and Withaferin A (j'''). Scale bar: 50 μ m. (k–k''') IF of incorporated BrdU (red), counterstained with DAPI (blue) at 56 hpf. Elevated cell proliferation in mutant epidermis (k', compare to wt (k)) is downregulated by Wortmannin (k''), Rapamycin (k'''), and Withaferin A (k'''). Scale bar: 100 μ m.

DOI: [10.7554/eLife.14277.027](https://doi.org/10.7554/eLife.14277.027)

The following source data is available for figure 9:

Source data 1. Source data for **Figure 9e**.

DOI: [10.7554/eLife.14277.028](https://doi.org/10.7554/eLife.14277.028)

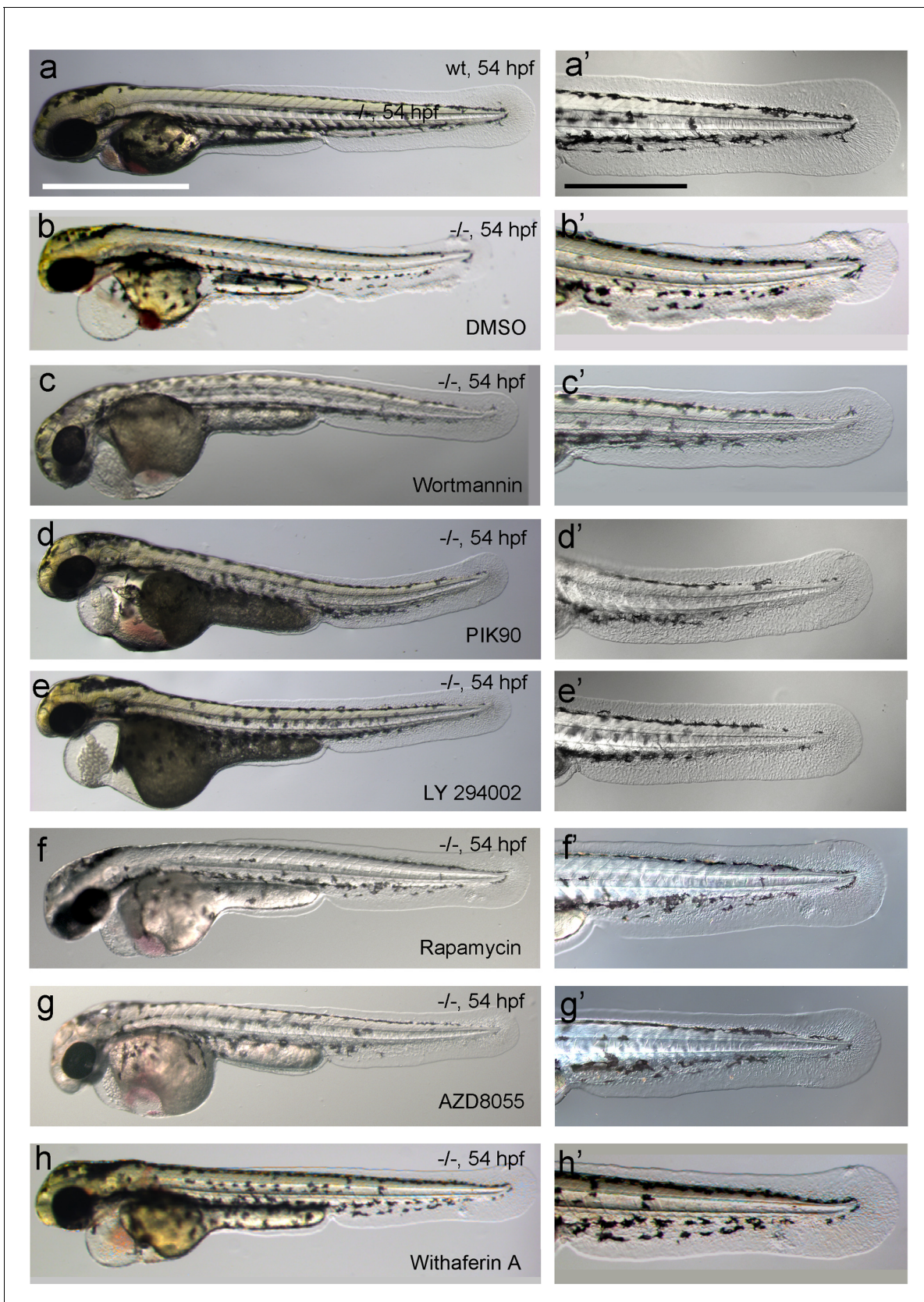


Figure 9—figure supplement 1. Chemical inhibition of PI3K, mTORC1 or NF κ B rescues the epidermal malignancies, but not the pericardial edema of *psoriasis* mutants. (a–h) Representative live images of *psoriasis* $-/-$ embryos at 54 hpf, treated with the PI3K inhibitors Wortmannin (1 μ M; c,c'), PIK90 (5 μ M; d,d'), LY 294002 (5 μ M; e,e'), Rapamycin (5 μ M; f,f'), AZD8055 (5 μ M; g,g') or Withaferin A (5 μ M; h,h'). Scale bars are shown in a and a'. *Figure 9—figure supplement 1 continued on next page*

Figure 9—figure supplement 1 continued

μM ; **d,d'**) and LY 294002 (25 μM ; **e,e'**), the mTORC1 inhibitors Rapamycin (1.1 μM ; **f,f'**) and AZD8055 (30 μM ; **g,g'**), and the NF κ B inhibitor Withaferin A (30 μM ; **h, h'**), as quantified in **Figure 9e**. Treatment with the different inhibitors of components of the PI3K-Akt-mTorC1-NF κ B pathway do not rescue the pericardial edema (**c–h**, compare to wt (**a**) and non-treated mutant (**b**)), but do rescue the epidermal malignancies of mutant embryos (**c'–h'**, compare to wt (**a'**) and non-treated mutant (**b'**)). Scale bars: 500 μm (**a**), 250 μm (**a'**).

DOI: [10.7554/eLife.14277.029](https://doi.org/10.7554/eLife.14277.029)

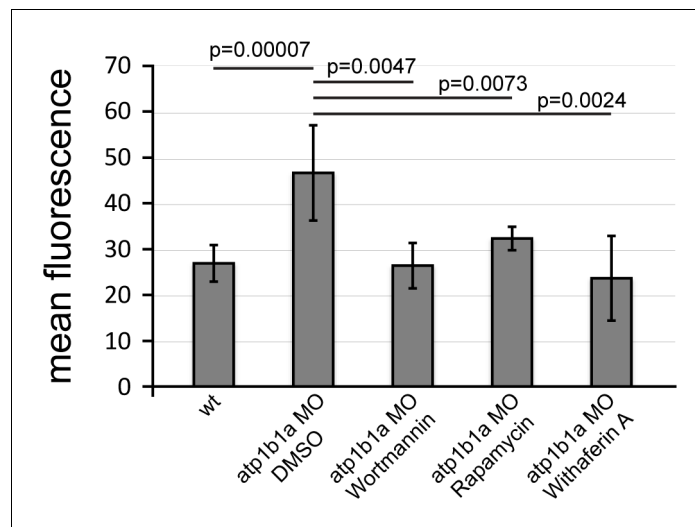


Figure 9—figure supplement 2. Quantification of NF κ B activity in wt embryos, *atp1b1a* morphants and *atp1b1a* morphants treated with Wortmannin, Rapamycin, and Withaferin A, as shown in **Figure 9i–i''''**. Mean fluorescence intensities of GFP in the posterior part of the tail fin were measured in maximum intensity projections of confocal images using ImageJ software. $n = 4–16$. Error bars represent standard deviations.

DOI: [10.7554/eLife.14277.030](https://doi.org/10.7554/eLife.14277.030)

The following source data is available for figure 9:

Figure supplement 2—Source data 1. Source data for **Figure 9—figure supplement 2**.

DOI: [10.7554/eLife.14277.031](https://doi.org/10.7554/eLife.14277.031)

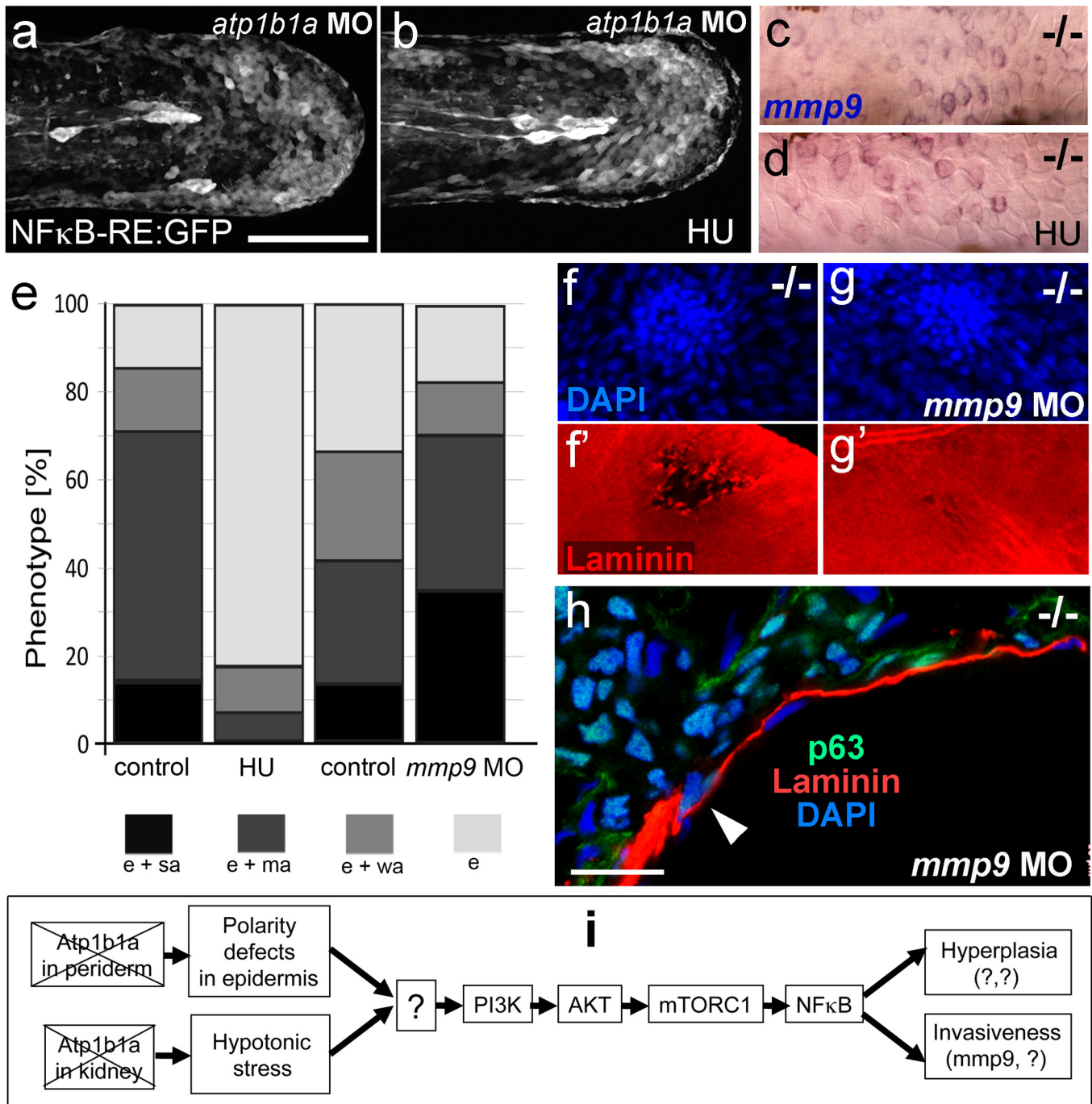


Figure 10. Blockage of cell proliferation results in the normalization of epidermal hyperplasia, whereas blockage of Mmp9 activity reduces epidermal invasiveness in *psoriasis* mutants. (a–b). Confocal images of GFP in the tail fin of live 48 hpf *atp1b1a* morphant *Tg(NFκB-RE:eGFP)* transgenics, showing that elevated NFκB activity in *atp1b1a* morphants (a) is not reduced by hydroxyurea treatment (b). For quantification, see **Figure 10—figure supplement 1**. (c–d) *mmp9* WISH of 54 hpf *psoriasis* mutants raised in hypotonic E3. Elevated *mmp9* expression in mutant epidermis (c) is not reduced by hydroxyurea (HU) treatment (d). (e) Quantification of the phenotypes of *psoriasis* mutants, either treated with 50 mM hydroxyurea or injected with *mmp9* MO, compared to their respective siblings. e, pericardial edema; wa, weak epidermal aggregates; ma, medium epidermal aggregates; sa, strong epidermal aggregates. n = 17–47. Similar results for each condition were obtained in two additional independent experiments. (f–g) *mmp9* knockdown alleviates basement membrane fragmentation. Laminin IF, counterstained with DAPI, in *psoriasis* mutants at 58 hpf, epidermal aggregates of comparable sizes. In the un-injected *psoriasis* mutant (f), the aggregate is associated with BM fragmentation, while the underlying BM is largely intact

Figure 10 continued on next page

Figure 10 continued

in the *psoriasis* mutant injected with *mmp9* MO (g). For more images and numbers, see **Figure 10—figure supplement 2**. (h) *mmp9* knockdown alleviates epidermal invasiveness. Laminin and p63 IF of transverse sections, counterstained with DAPI, through the yolk sac of a *psoriasis* mutant (58 hpf) injected with *mmp9* MO. The basement membrane is largely intact (arrowhead to small remaining region with thinner basement membrane), and p63 keratinocytes are confined to the epidermal compartment above the basement membrane. For un-injected mutant and wt controls, see **Figure 2i,j**. (i) Diagram of the identified pathway in which the two required non-cell-autonomous effects caused by loss of *Atp1b1a* in periderm and osmoregulatory organs converge in basal cells. The pathway subsequently diverges downstream of NFκB to mediate overgrowth versus invasiveness of transformed keratinocytes. Question marks indicate components that have not yet been identified. For details, see text.

DOI: [10.7554/eLife.14277.032](https://doi.org/10.7554/eLife.14277.032)

The following source data is available for figure 10:

Source data 1. Source data for **Figure 10e**.

DOI: [10.7554/eLife.14277.033](https://doi.org/10.7554/eLife.14277.033)

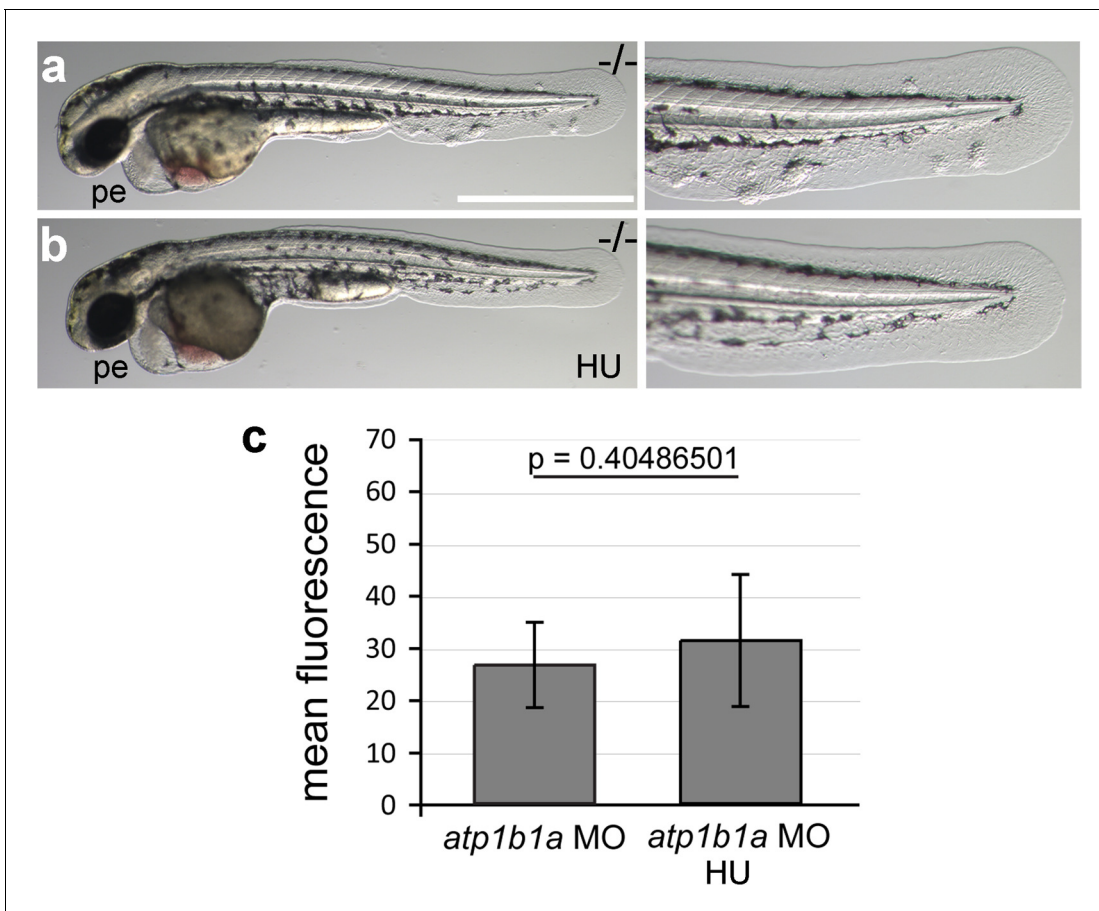


Figure 10—figure supplement 1. Morphology rescue of *psoriasis* mutant upon treatment with hydroxyurea and quantification of the non-alleviating effect of the treatment on NF κ B activity in embryos as shown in **Figure 10a,b**. (a–b) Live images of a 54 hpf *psoriasis* mutant treated with 50 mM hydroxyurea (HU) in E3 from 34 hpf onwards (b) and control mutant raised in E3 (a). Hydroxyurea does not rescue the pericardial edema (a,b), but blocks epidermal aggregate formation (a',b'). (c) Mean fluorescence intensities of GFP in the posterior part of the tail fin were measured in maximum intensity projections of confocal images using the ImageJ software. $n = 7-8$. Error bars represent standard deviation.

DOI: [10.7554/eLife.14277.034](https://doi.org/10.7554/eLife.14277.034)

The following source data is available for figure 10:

Figure supplement 1—Source data 1. Source data for **Figure 10—figure supplement 1**.

DOI: [10.7554/eLife.14277.035](https://doi.org/10.7554/eLife.14277.035)

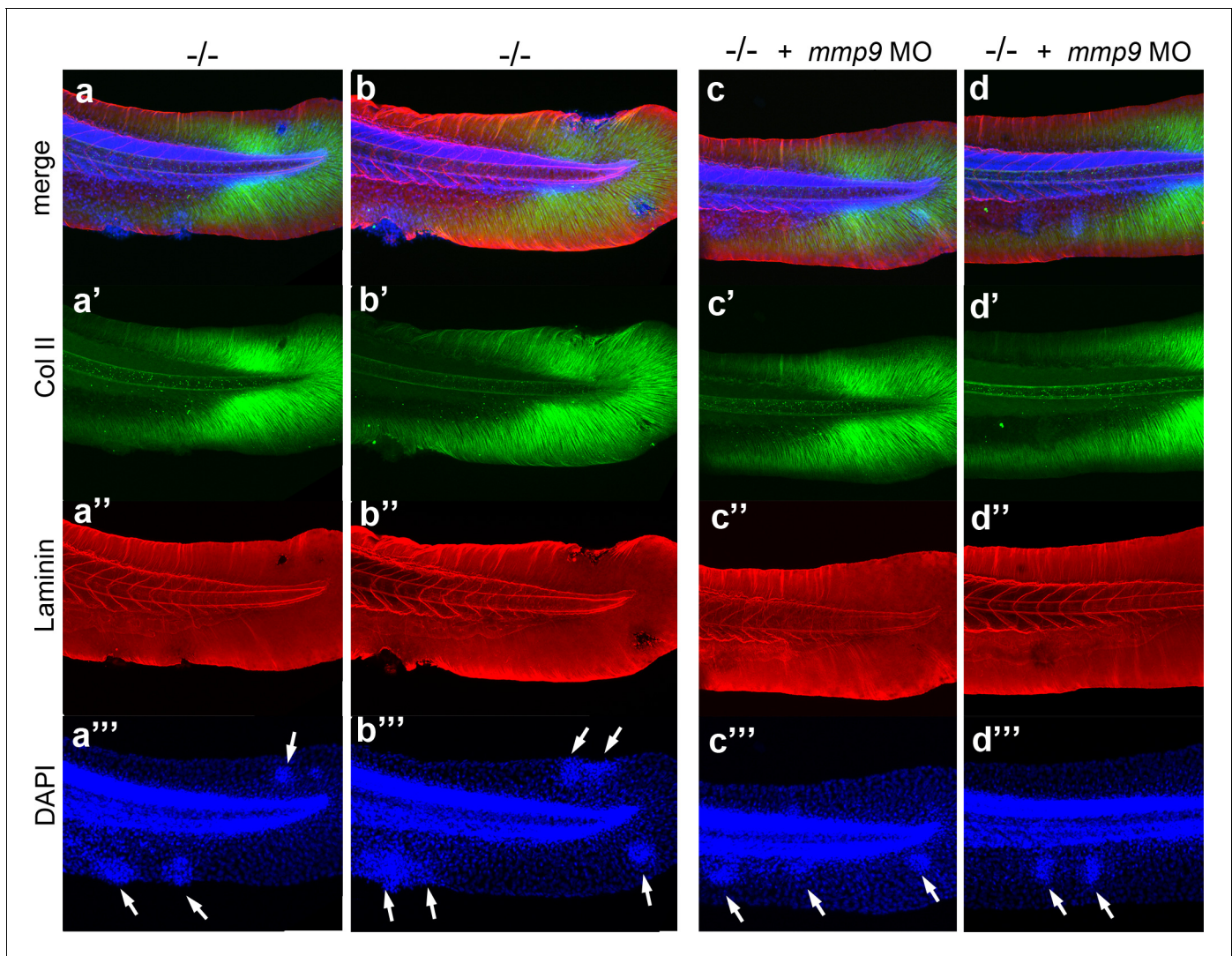


Figure 10—figure supplement 2. *mmp9* knockdown alleviates epidermal invasiveness. Examples of whole mount immunofluorescence of laminin (red) and type II collagen (green) of the tail fin of 58 hpf *psoriasis*^{-/-} embryos (a,b) and *psoriasis*^{-/-} ; *mmp9* MO embryos (c,d), counterstained with DAPI (blue). Actinotrachia disassembly (a'–d') and basement membrane disruption (a''–b'') observed below epidermal aggregates (arrows in a'''–d''') are strongly reduced upon knockdown of *mmp9*. In total (5 embryos examined per condition), 5/22 medium-sized fin fold aggregates were associated with BM fragmentation in *mmp9* MO-injected mutants, compared to 19/19 in un-injected mutant controls.

DOI: [10.7554/eLife.14277.036](https://doi.org/10.7554/eLife.14277.036)